Chapter

Recent Advancements in the Hole-Drilling Strain-Gage Method for Determining Residual Stresses

Emilio Valentini, Lorenzo Bertelli, Alessio Benincasa and Simone Gulisano

Abstract

The hole-drilling Strain-Gage method is a widely used and cost-effective technique for the evaluation of residual stresses. The test method is standardized by ASTM E837-13a, which defines the scope, measurement range, minimum requirements of instrumentation, test procedure, and algorithms and coefficients for the computation of uniform and non-uniform stress distribution. However, the standardized test method presents some limitations regarding the scope and measurement range; moreover, some typical errors involved in the measurements are not taken into account, i.e., errors due to the hole eccentricity, the local plasticity, the intermediate thickness, and the hole-bottom chamfer, which can affect the results in some cases. Also, the standard does not provide the user with a complete guide regarding the evaluation of the uncertainty connected with this type of measurement. The paper presents a more general approach that allows the correction of some errors and overcomes and some limitations of the ASTM E837-13a test method, contributing to greater accuracy of the test results.

Keywords: residual stress, hole-drilling method, ASTM E837, eccentricity error, local plasticity effect, intermediate thickness, hole-bottom chamfer, uncertainty evaluation

1. Introduction

The hole-drilling method is one of the most cost-effective and simple methods to evaluate the residual stresses present in typical industrial workpieces. Those stresses are induced in the material whenever it is subjected to mechanical or thermal treatments and their effect is often a requirement for the best working condition of the workpiece. Therefore, in most industrial applications, it is very important to have an accurate estimation of the magnitude of the residual stresses particularly where they could represent a critical aspect for the integrity of a component. Nowadays, different methods can be adopted in order to measure the residual stresses in a specimen, and they differ in many features, such as, the depth of investigation or the type of material.

The hole-drilling method represents an interesting solution for the measurement of residual stress. Following the instructions reported in the ASTM E837-13a standard [1], a small hole is made in the center of a strain gage composed of a minimum

of three grids. The method requires a sequence of drilling steps to be performed, at the end of which the relaxed strains are acquired from the rosette. The data are then used to calculate the magnitude and the direction of the residual stresses using the calibration coefficients supplied by the standard.

The field of application of the method is wide-ranging and comprises typical mechanical engineering sectors, such as, metallurgy, automotive, aerospace and energy. Hole-drilling measurements can be performed in metal, composite and polymer materials [2]. The method also allows the test to be performed in different conditions, both in a laboratory and on field [3, 4].

According to the ASTM standard, the acquired strains are used for the calculation of residual stress applying the appropriate calibration coefficients depending on the thickness of the workpiece and the type of calculation (uniform or non-uniform). In the case of non-uniform distribution, the evaluation of residual stresses is based on the application of the integral method introduced by Schajer [5, 6].

Standard ASTM E837-13a reports the calibration coefficients for three types of standardized rosette (type A, type B and type C), specifying the related geometric dimensions. Unfortunately, the geometric dimensions of many commercial rosettes do not match those of standard rosettes, and in these cases, the calibration coefficients must be recalculated, taking into account the actual dimensions.

Beghini et al. [8, 9] introduced the influence function approach for a blind hole in a thick workpiece. The strain field was computed starting from a database of numerical solutions, implementing a specific geometric configuration in which the components of eccentricity are merely introduced as the geometry parameters rather than being considered as a source of error. This approach is more extensive with respect to the integral method and includes a parametric description of the strain gage rosette. Using the influence function approach, it is possible to include in the calculation different influence parameters such as the thickness of the specimen or a small bottom chamfer that could be present in the drilled hole.

The eccentricity is the possible error that can be made by the operator during the hole-drilling test, due to misalignment between the drilled hole and the strain gage circle. The ASTM standard sets the limit of 0.004 D (where D is the diameter of the gage circle) as the maximum error of eccentricity. If the actual eccentricity value is measured after drilling, the correction of the eccentricity error will increase the accuracy of the measurements. With this correction, the measurements could be acceptable even in cases where the limit set by the standard is exceeded. Over the years, several approaches have been proposed for the correction of this effect [8–14].

Regarding the thickness of the workpiece under testing, the ASTM standard does not include any instructions for residual stress evaluation for intermediate thickness values ranging from 0.2D to D, where D is the diameter of the strain gage circle. Nevertheless, industrial reality presents a lot of cases where this condition exists, such as with metal sheets or automotive parts. To solve this problem, Abraham and Schajer [15] and Beghini et al. [16] presented correction methods with related calibration coefficients.

The calibration coefficients provided by the ASTM E837-13a standard refer to a cylindrical hole with a flat bottom. Sometimes, end mills used in drilling have a small chamfer that produces a hole that is not perfectly cylindrical, with consequent errors in the measurement of relaxed deformations. To obtain measurements that are more accurate, it is therefore necessary to use calibration coefficients that consider the presence of the chamfer at the bottom of the hole. This source of error will be examined in greater detail, considering the proposed calibration coefficients to take this effect into account [17–19].

Sometimes, the hole-drilling method is used on components that have high residual stress values, comparable with the yield stress of the material. Drilling a hole locally modifies the geometry of the specimen and the stresses around the hole increase by the concentration factor of the discontinuity. It is possible to adopt a stress correction methodology for a uniform stress field and the blind hole case [20–22].

Evaluation of measurement-related uncertainties is also analyzed. Although the ASTM E837 standard does not include a detailed method for the uncertainty evaluation, some scientific works define the main sources of uncertainty and propose some approaches for expressing uncertainty in the case of uniform and non-uniform residual stresses [23–27].

Lastly, the paper shows an application of the hole-drilling method on a known-stress testing configuration obtained using a 4-point bending stress condition. The stresses are evaluated taking into account the effect of the correction of some of the errors described above, and then compared with the expected bending stress distribution. Finally, measurement uncertainty is evaluated with the same calculated stress distribution.

2. Improvements in procedure and devices used to perform hole-drilling residual stress measurements

The ASTM E837 standard provides several details about the testing procedure for strain-gage hole-drilling measurements, including the requirements for the entire measurement chain used for performing the test. A typical hole-drilling measurement chain is composed of two parts: the device used for drilling the hole and the strain gage amplifier used for the acquisition of strains.

The drilling sequence is performed using a drilling technology that minimizes the machining-induced residual stresses at the hole boundary. For this reason, the standard requires that drilling speed remains in the range of 20,000–400,000 rpm: this drilling speed can be obtained using either a high-speed air turbine or an electric motor.

The hole can be made using center-hole drilling or the orbital drilling technique. The orbital method has the advantages of adjusting the diameter of the hole by choosing the offset, of determining a more regular flow of chips and of reducing the geometric dimensions of the small chamfer at the bottom edge of the hole (**Figure 1b**).

The ASTM standard defines some features of a hole-drilling device and the fundamental requirement that the drilling depth must be accurately controlled. The uncertainty of the depth increments, required by the standard, depends on the size of the strain gage rosette used during the measurement and needs to be lower than $\pm 0.004D$. The depth accuracy requirement is essential in the case of a non-uniform stress profile where the hole is made using a step-by-step drilling sequence. For example, when using a rosette with a diameter D of approximately 2.56 mm, the depth uncertainty must be lower than ± 10 μm. This requirement can be difficult to obtain using a manual drilling device.

The use of an automatic drilling system instead of a manual system significantly increases the accuracy of the measurements. The automatic systems use an electronic device and dedicated acquisition and control software; they allow accurate control of the positioning of the end mill, necessary to meet the accuracy requirements of the standard and reducing the total testing time (**Figure 2**).

When maximum accuracy is required in depth increments, it is advisable to use an LVDT sensor, connected to the mechanical body of the drilling unit, which

Figure 1.
(a) LVDT sensor installed on the drilling device and (b) orbital drilling slide.

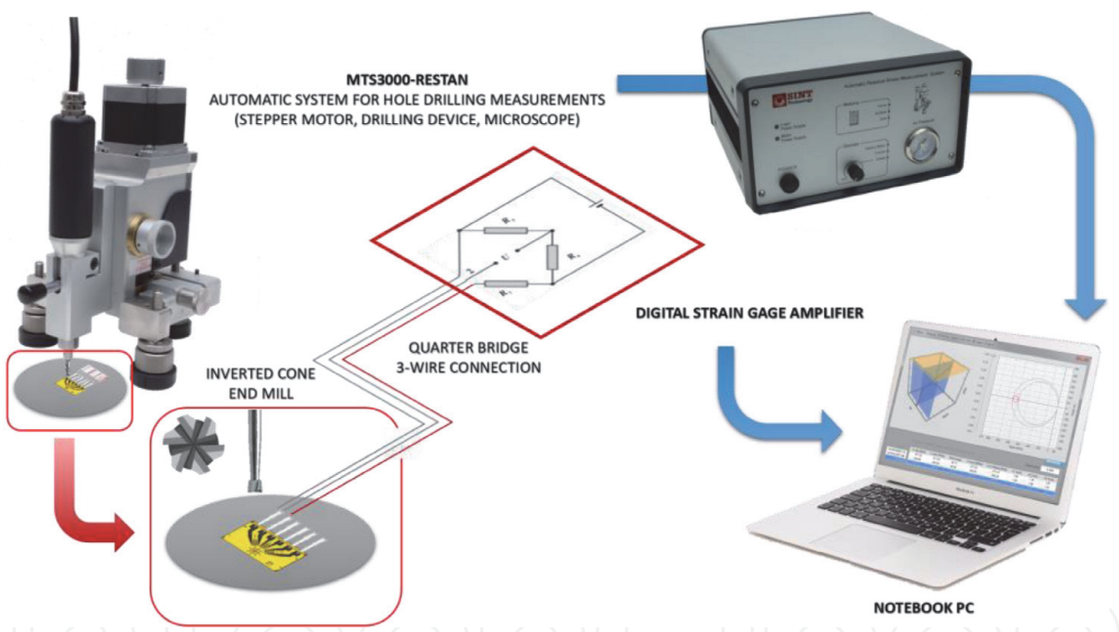

Figure 2.
Hole drilling measurements: typical automatic measuring device (MTS3000-Restan system—SINT Technology).

allows an accuracy of few microns (**Figure 1a**). An automatic system allows a higher number of drilling steps, a uniform feed rate and a fixed stabilization time. Moreover, it can be controlled remotely, minimizing operator presence near the drilling unit [2]; this is particularly important in the case of hole-drilling measurements on polymeric or composite materials.

To obtain accurate measurements, it is very important to establish the point that corresponds to the "zero" cutter depth. The standard identifies it as the point at which the end mill begins to lightly scratch the surface of the workpiece, during slow advance drilling. It is clear that the quality of the results of this process greatly depends on the skill of the operator who carries out the measurements and may not be very accurate.

In the case of tests on conductive materials, it is possible to use the electrical contact technique that identifies the contact when the electrical connection occurs

between the tip and the surface of the workpiece. Alternatively, it is advisable to automatically measure the strain variation during the detection of the zero depth surface; when the end mill slowly touches the material surface, the strain gages detect the strain variation and the system immediately stops the drilling operation.

3. Advancements in residual stress calculation

After acquisition of the relaxed strain values, the residual stresses need to be evaluated. First of all, it is necessary to choose between blind-hole and through-hole calculation and between uniform or non-uniform stress distribution along the depth. When the residual stress value is uniform along the depth, the ASTM E837-13a standard specifies that the formulas described in Section 8 of the standard be used. The standard suggests assuming the stress to be uniform only when prior information about the expected stress field is available or if a representative size of the magnitude of the residual stress is required.

Typical applications generally exhibit a non-uniform state of residual stresses. In this case, it is necessary to follow the instructions reported in Section 9 of ASTM E837-13a for the calculation of residual stresses along the depth. The standard provides the calibration matrices, derived by the integral method, that must be multiplied with the acquired strains to derive the stress values. The matrix coefficients, corresponding to each calculation depth, are dimensionless and almost independent of the material [1].

For the sake of simplicity, only the equation for the calculation of the combination stress P is shown below.

$$\left(\overline{\boldsymbol{a}}^T\overline{\boldsymbol{a}} + \boldsymbol{\alpha}_P\overline{\boldsymbol{c}}^T\overline{\boldsymbol{c}}\right)\cdot\boldsymbol{P} = \frac{E}{1+\nu}\overline{\boldsymbol{a}}^T\boldsymbol{p} \tag{1}$$

It is important to point out that dependence of the stresses on the Poisson's ratio, as shown in Eq. 1, is simplified [13].

All the coefficients reported in the calibration matrices A and B, for a non-uniform stress field, are strictly related to the nominal hole diameter (D_N) of 2 mm. If the diameter of the drilled hole (D_0) differs from the nominal value, each matrix coefficient reported in the standard needs to be corrected using Eq. 2 reported below:

$$\overline{a}_{j,kNEW} = \left(\frac{D_0}{D_N}\right)^2\overline{a}_{j,k} \tag{2}$$

The dependency of the coefficients of the calibration matrix on the drilled hole diameter, as expressed in Eq. 2, is approximated as explained by Alegre et al. [7]. For example, using a rosette with a strain gage circle diameter (D) of 5.13 mm, the nominal hole diameter (D_N) is equal to 2 mm and the allowed diameter of the drilled hole (D_0) can vary from 1.88 to 2.12 mm. The ratio $(D_0/D_N)^2$ ranges between 0.88 and 1.12.

Recently, some developments have been carried out to overcome the limits of the ASTM E837 standard previously described and to take into account other parameters affecting the results that are not considered in the standard.

Beghini et al. [8, 9] of the University of Pisa introduced a generalized integral method based on the analytical definition of influence functions. The method is substantially an evolution of the Integral Method and it also overcomes the limitation of the ASTM E837 standard regarding the maximum allowable value of

Parameters	Limitations	
	ASTM E837 for non-uniform stress field calculation [1]	**Generalized integral method, based on the influence functions [8, 9]**
Hole diameter	Approximated correction if hole diameter differs from the nominal value used for the evaluation of the calibration coefficients	No limitation
Poisson's ratio	Approximated correction if Poisson's ratio differs from the value used for the evaluation of the calculation coefficients	Not applicable if outside the range 0.25–0.45
Rosette geometry	Fixed only for the strain gage rosette (A, B and C) reported in the standard.	Variable. Strain gage circle diameter (D), grid length (G_L) and width (G_W) can be used as input parameters
Hole eccentricity radius	Eccentricity correction is not included. Is considered acceptable if lower than 0.004D	No limitation
Workpiece thickness	<0.2D thick (uniform stress) >1.0D thin (uniform/non-uniform stress)	No limitation
Hole-bottom chamfer	Not considered	Considered (for a specific end mill geometry)

Table 1.
Comparison between the limitations of the ASTM E837-13a method and those of the generalized integral method based on the influence functions.

eccentricity. Using the Influence functions approach, it is also possible to include the real dependency of the Poisson's ratio and the diameter of the drilled hole on the calculated stress. In detail, the proposed methodology is based on analytical influence functions relating the measured relieved strains to the residual stress by means of integral equations. By processing the results of accurate finite element simulations, continuous analytical influence functions are produced.

The generalized integral method is more universal compared to the ASTM E837 standard and is currently the most suitable to include the influence parameters not considered in the standard and therefore to overcome its limitations. With this calculation method, it is possible to take into account other influence parameters, such as hole bottom chamfer and intermediate thickness.

Table 1 provides a comparison of the limitations of the ASTM E837 standard and of the generalized integral method based on the influence functions.

4. Generalized integral method

The ASTM E837 standard (Section 9.3) uses the integral method, including the Tikhonov regularization, to calculate non-uniform residual stresses. The residual stresses for each hole depth j are computed by solving the following matrix equations:

$$\left(\overline{\boldsymbol{a}}^T\overline{\boldsymbol{a}} + \alpha_P \boldsymbol{c}^T\boldsymbol{c}\right)\cdot \boldsymbol{P} = \frac{E}{1+\nu}\boldsymbol{p} \tag{3}$$

$$\left(\overline{\boldsymbol{b}}^T\overline{\boldsymbol{b}} + \alpha_Q \boldsymbol{c}^T\boldsymbol{c}\right)\cdot \boldsymbol{Q} = E\boldsymbol{q} \tag{4}$$

$$\left(\overline{\boldsymbol{b}}^T\overline{\boldsymbol{b}} + \alpha_T \boldsymbol{c}^T\boldsymbol{c}\right)\cdot \boldsymbol{T} = E\boldsymbol{t} \tag{5}$$

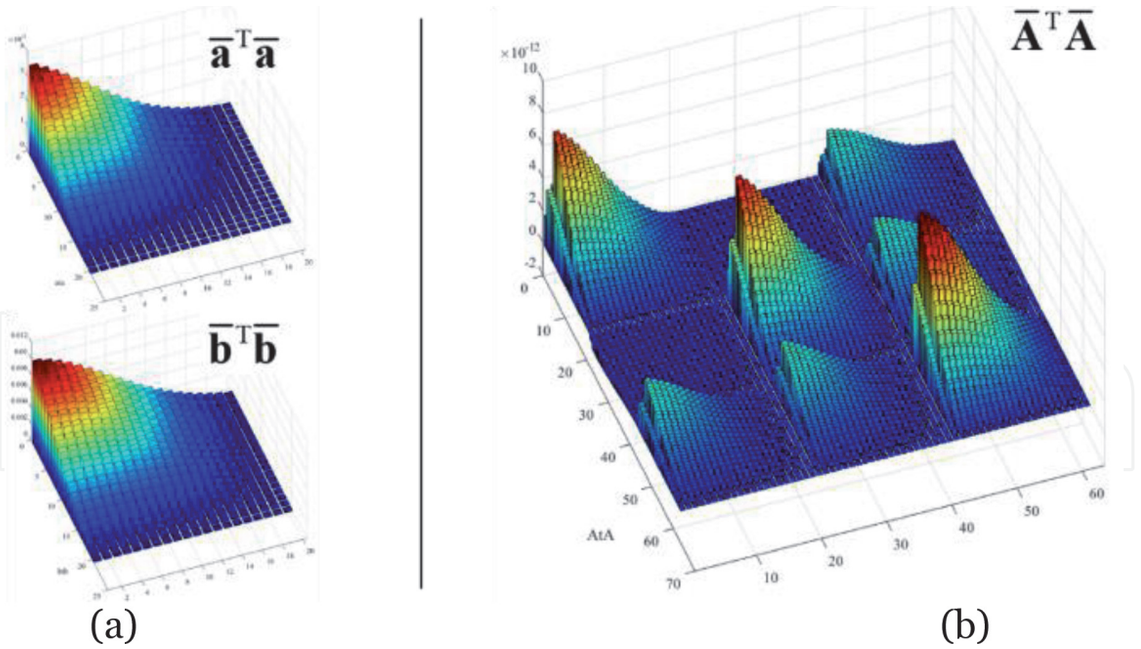

Figure 3.
(a) Two calibration matrices $\overline{a}$ and $\overline{b}$ for the ASTM E837 test method. (b) Calibration matrix A, composed of 9 blocks, for the generalized integral method.

Eqs. (3)–(5) are applicable only in the case of concentric holes, where it is possible to decouple the strain components.

Beghini et al. [8, 9] and, more recently, Barsanti et al. [13] extended the Integral Method by including a correction for the eccentricity of the hole with respect to the strain-gage rosette.

For this general problem, no symmetry can be used and no advantage is obtained by separating stress and relieved strain in equibiaxial and shear components. Therefore, the problem will be solved using the Cartesian reference system of the rosette.

The relationship between the strain and the stress can be re-written as reported below:

$$\left(\overline{\boldsymbol{A}}^{\boldsymbol{T}}\overline{\boldsymbol{A}} + \boldsymbol{\alpha}\boldsymbol{C}^{\boldsymbol{T}}\boldsymbol{C}\right) \cdot \boldsymbol{S} = \boldsymbol{E}\overline{\boldsymbol{A}}^{\boldsymbol{T}}\boldsymbol{e} \tag{6}$$

where $\mathbf{S} = \left(\sigma_x^{(1)}, \sigma_y^{(1)}, \tau_{xy}^{(1)}, \ldots, \sigma_x^{(k)}, \sigma_y^{(k)}, \tau_{xy}^{(k)}\right)^T$ is the vector of the stress components; $\boldsymbol{e} = \left(\varepsilon_1^{(1)}, \varepsilon_2^{(1)}, \varepsilon_3^{(1)}, \ldots, \varepsilon_1^{(k)}, \varepsilon_2^{(k)}, \varepsilon_3^{(k)}\right)^T$ is the vector of strain reading; $\overline{\boldsymbol{A}}$ = generalized matrix of calibration coefficients.

$\boldsymbol{S}$ and $\boldsymbol{e}$ have different sizes compared to the standard ASTM E837 approach. In this different formulation, the two vectors are defined using a $3k \times 1$ arrangement with a block structure of 3-elements.

The matrix $\overline{\boldsymbol{A}}$ has a size of 3 k × 3 k and implicitly includes the dependency of the calculated stress on the hole diameter, type and dimension of the strain gage rosette (including the gage circle diameter, length and width of the strain grids), Poisson's ratio, eccentricity and, if applicable, hole bottom chamfer and thickness of the workpiece.

The equations reported above include also the Tikhonov regularization, as in the ASTM E837 standard.

As for the strain and the stress components, also the new matrix of calibration coefficients is defined for blocks of 3 × 3 elements as reported below:

$$\overline{A} = \begin{bmatrix} A_{11}^{(11)} & A_{12}^{(11)} & A_{13}^{(11)} & & & 0 & 0 & 0 \\ A_{21}^{(11)} & A_{22}^{(11)} & A_{23}^{(11)} & \cdots & \cdots & 0 & 0 & 0 \\ A_{31}^{(11)} & A_{32}^{(11)} & A_{33}^{(11)} & & & 0 & 0 & 0 \\ & \vdots & \ddots & . & & & \vdots & \\ & \vdots & . & \ddots & & & \vdots & \\ A_{11}^{(k1)} & A_{12}^{(k1)} & A_{13}^{(k1)} & & & A_{11}^{(kk)} & A_{12}^{(kk)} & A_{13}^{(kk)} \\ A_{21}^{(k1)} & A_{22}^{(k1)} & A_{23}^{(k1)} & \cdots & \cdots & A_{21}^{(kk)} & A_{22}^{(kk)} & A_{23}^{(kk)} \\ A_{31}^{(k1)} & A_{32}^{(k1)} & A_{33}^{(k1)} & & & A_{31}^{(kk)} & A_{32}^{(kk)} & A_{33}^{(kk)} \end{bmatrix} \quad (7)$$

Figure 3 compares the visual interpretation of the calibration matrices of the ASTM standard and that of the new generalized calibration matrix.

5. The main sources of errors and limits of applicability in the hole drilling method

The hole-drilling method has some typical sources of error that can influence the accuracy of the measurements. The ASTM E837 standard identifies the maximum values of these errors for the validity of the test (limits of applicability) without providing recommendations on how to correct them, as reported in **Table 2**.

Some of these errors, for example, eccentricity and hole bottom chamfer, can be generated by external sources such as the operator, testing condition or the drilling process. In other cases, the limits of applicability are directly connected with the test method, as in the case of intermediate thickness of the specimen or the local plasticity effect.

Table 2 also shows the bibliographic sources dealing with possible methods of error correction. The cases of uniform and non-uniform stress distribution are analyzed. In the case of uniform stress distribution, both the thin workpiece and the thick workpiece are considered.

The following sections examine the errors mentioned above in more detail and consider possible corrections.

Typical source of error	ASTM E837 limits of applicability	Suggested correction		
		Uniform		Non-uniform
		Thin	Thick	/
Hole eccentricity	Eccentricity radius within 0.004D	[12] [10, 11]	[8, 9] [10, 11]	[8, 9, 13, 14] [10, 11]
Intermediate thickness(s)	Thickness $s \leq 0.2D$ or $s \geq 1.0D$	[8, 9, 15, 16]		[8, 9, 16]
Hole-bottom chamfer	Not provided	Not applicable	[8, 9, 17]	[8, 9]
Local plasticity	Magnitude of the stresses ≤50% of σ_Y—Thin specimen ≤80% of σ_Y—Thick specimen	/	[20]	/

Table 2.
Typical sources of errors, ASTM E837 limit of applicability and current state-of-the-art of correction methodologies.

6. Eccentricity error: description and possible corrections

The eccentricity between the drilled hole and the strain gage circle greatly influences the strain measurements. The ASTM standard requires a near perfect concentricity between the drilled hole and the rosette and prescribes an allowable eccentricity value that depends on the dimension of the strain gage rosette (0.004D). Using a standard rosette with a gage circle diameter D = 5.13 mm, the maximum allowable eccentricity is 0.02 mm. This limit increases (0.04 mm) or decreases (0.01 mm) using bigger (approx. D = 10.26 mm) or smaller types of rosette (approx. D = 2.56 mm).

As shown in **Figure 4**, the eccentricity error is influenced by the eccentricity coordinates e_x and e_y and by the parameters of the strain gage rosette (D, G_L and G_W). The type B rosette generally shows a higher sensitivity to eccentricity errors compared to type A rosettes; this can be explained by the orientation of the gage grids, which are concentrated only in the first quadrant (0°, 45°, 90°), instead of in the first and third quadrant (0°, 90°, 225°).

For these reasons, the correction of eccentricity errors requires accurate determination of the position of the drilled hole in the reference system of the strain gage rosette; eccentricity can be measured by a special procedure using the drilling system microscope. Using a digital microscope, the eccentricity coordinates can be easily obtained by image analysis techniques.

As shown in **Figure 5**, the sensitivity of the grids is directly influenced by the hole eccentricity. When the eccentricity has the same direction as the grid, if the hole is closer to the grid the absolute value of the relaxed strain is greater. On the contrary, if the eccentricity has a transverse direction with respect to the grid, then a portion of the grid has a greater sensitivity, while the other portion has a lower sensitivity; this implies, by symmetry, that the error is almost compensated [13].

The eccentricity correction can be done using strain gage rosettes with special configurations or using correction algorithms.

The studies of Beghini et al. [10] and of Nau et al. [11] introduced the correction of eccentricity using a special six-grid rosette and an eight-grid rosette respectively. Both the rosettes are produced by HBM and make it possible to compensate the first-order of eccentricity error. However, the corrections based on special strain gage geometries do not correct the higher order eccentricity errors (higher than

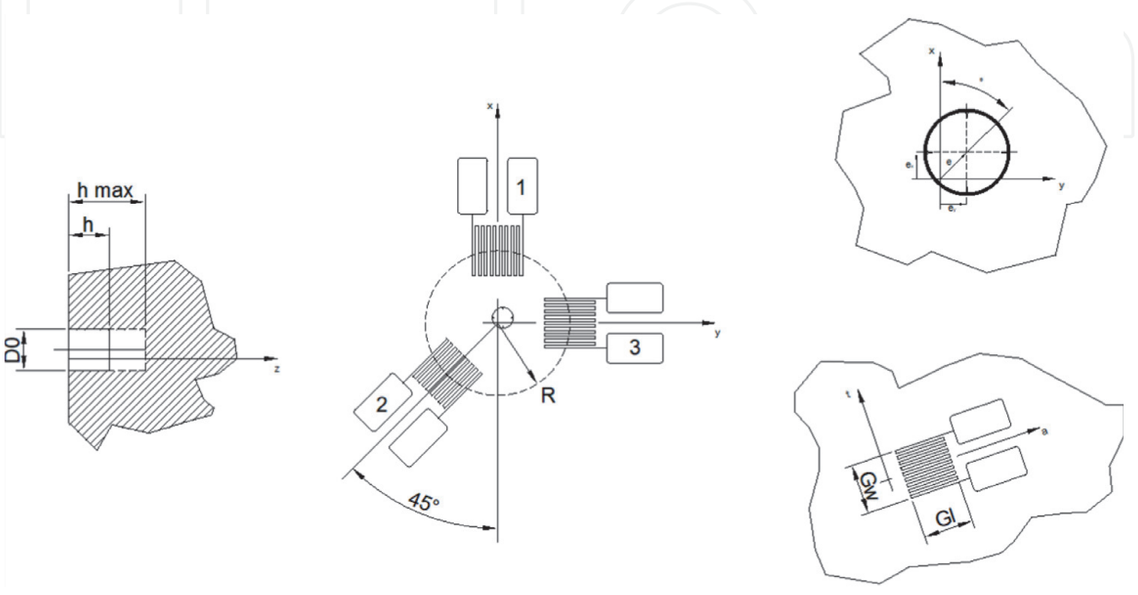

Figure 4.
Eccentricity in hole-drilling measurements.

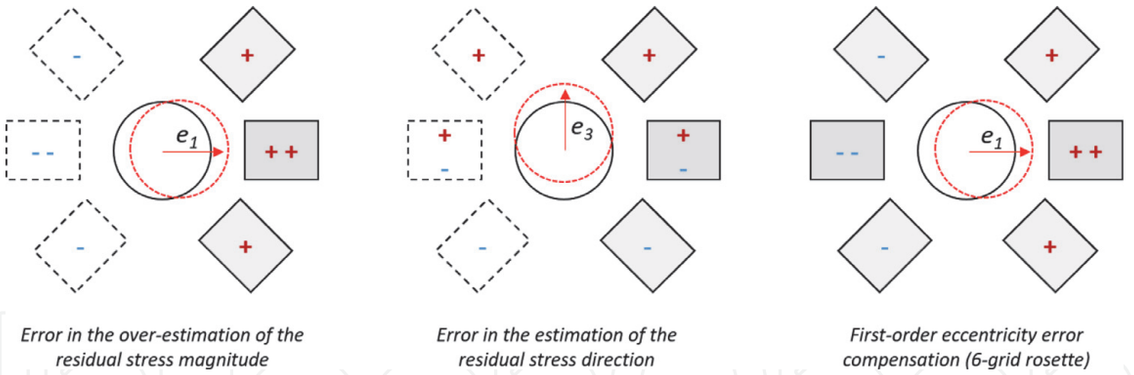

Figure 5.
Grid sensitivity to longitudinal and transversal eccentricity and first-order eccentricity error compensation using a 6-grid rosette.

0.2 mm), for which rosettes are required with bigger dimensions, a higher number of grids and higher costs.

Regarding the correction algorithms, the first solution was provided analytically by Ajovalasit et al. [12] for uniform stress in thin workpieces.

Beghini et al. [8, 9] provided a complete solution for blind holes using a generalized integral method based on the influence functions for non-uniform calculations (Section 4). According to this approach, the strain field is computed starting from a database of numerical solutions in which the eccentricity is simply introduced as a geometry parameter; this has the advantage of taking into account the whole effect of eccentricity. Recently, Barsanti et al. [13] proposed a simplified approach for the analytical correction of the first-order eccentricity errors in calculated stresses.

Peral et al. [14] has also proposed a correction approach applied to acquire strains.

7. Intermediate thickness limitation: description and possible correction

The ASTM E837 method defines the application ranges concerning the thickness of the workpiece under testing. The measurements can be carried out on "thin" or "thick" workpieces, the thickness of which depends on the size of rosette. For a "thin" workpiece, the thickness should be less than 0.20D (for type A and type B rosettes) and the stresses are evaluated according to the "uniform stress calculation". For a "thick" workpiece the thickness should be greater than 1.0D (for type A and type B rosettes) and the standard provides the calculation methods for uniform and non-uniform stress distributions.

The range of thicknesses between 0.2D and 1.0D, defined as intermediate thickness, is outside the scope of the ASTM standard. Using a strain gage rosette with a gage circle diameter D = 5.13 mm, the intermediate thickness is identified in the range between 1 and 5.13 mm. Clearly, on varying the diameter of the strain gage circle, also the range of the intermediate thickness varies.

Unfortunately, intermediate thickness is common in several types of engineering applications, as in aerospace, motor sports and energy production.

This limitation in the ASTM standard can be explained by analysis of the behavior of stress response if a hole is made in an intermediate thickness specimen.

In the case of thick workpieces ($s > 1.0D$) the influence coefficients are independent of the thickness and they can be obtained by an FE model in which the hole is produced in a virtually semi-infinite body. In the case of thin workpieces

($s \leq 0.2D$) the plane stress solution holds, the in-depth residual stress gradient is neglected and the through-hole method is applied; the influence coefficients for the thin plates can be directly deduced by Kirsch's solution of a membrane with a circular hole.

For the intermediate thickness case ($0.2D < s \leq 1.0D$), out-of-plane bending occurs (**Figure 6**) and this affects the calibration coefficients ***a*** and ***b*** defined in the ASTM standard. The calibration coefficients will depend directly on the workpiece thickness s, which becomes the new parameter.

A preliminary solution to this effect for the case of a uniform stress field was proposed by Abraham and Schajer [15]. They provide an analytical model of the calibration coefficients $\bar{a}, \bar{b}$ for intermediate thickness, as a function of workpiece thickness, hole diameter and hole depth.

Recently, Beghini et al. [16] described a procedure for the evaluation of non-uniform residual stress for the intermediate thickness range. The authors define two equations (one for the coefficients $\bar{a}_{j,k}$ and one for the coefficients $\bar{b}_{j,k}$), that adequately reproduce the thickness dependency of all the ASTM E837 calibration coefficients, for calculation of non-uniform stresses (**Figure 7**).

As reported in **Figure 7**, the dependency of the thickness is greater in the first part of the intermediate area (from 0.1D to 0.5D) and is less if the thickness is higher.

Moreover, a recent development of the generalized integral method based on the Influence Functions [8, 9] has introduced a new database of numerical solutions that takes thickness into account as an input parameter. The numerical database is

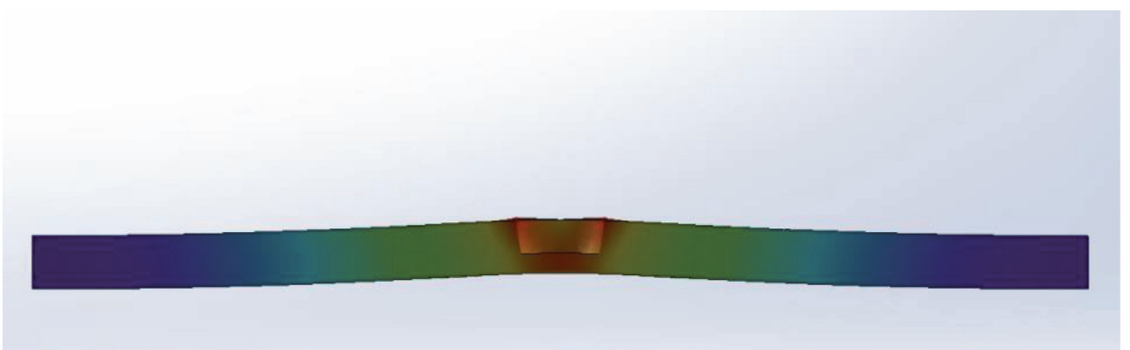

Figure 6.
Localized bending caused by hole-drilling in an "intermediate" thickness specimen.

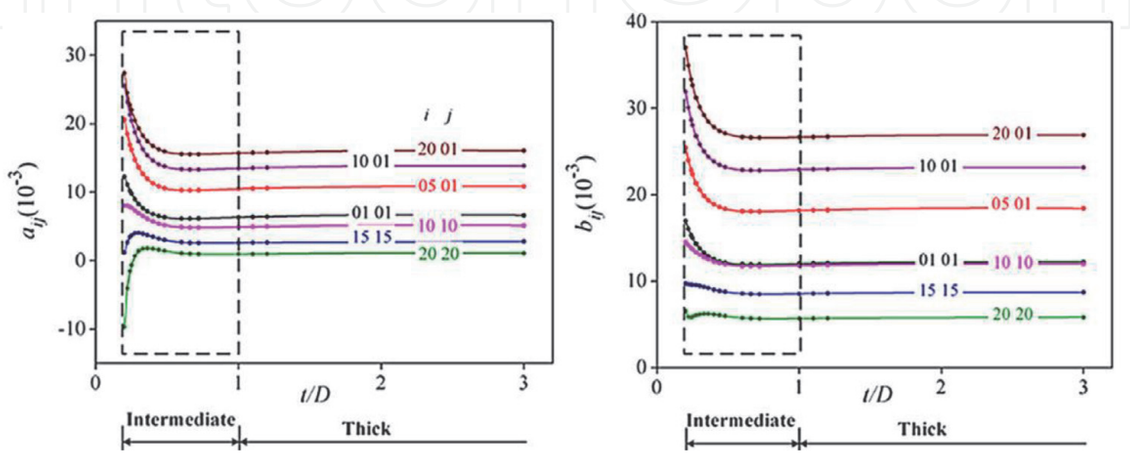

Figure 7.
Calibration coefficients as a function of plate thickness: for a_{ij} (left) and for b_{ij}, (right) coefficients in the matrices (from Beghini et al. [16]).

based on 5 different thicknesses (2.7 D, 1.0 D, 0.6 D, 0.3 D, 0.2 D); once the thickness is defined, the displacements are interpolated between the two closest available thickness values.

8. Hole bottom-chamfer error: description and possible correction

The hole-drilling method is based on the theoretical assumption that the drilled hole is perfectly cylindrical at any drilling increment. Perfect cylindrical holes are used in finite element models, by various authors, for the determination of the calibration coefficients.

The ASTM standard makes some recommendations regarding the geometry of the end mill in relation to both the radial clearance angles of the cutting edges on the end face of the cutting tool (<1°) and the taper angle (<5°). These requirements were introduced by the standard in order to avoid any ambiguity in determination of the depth and measurement of the hole diameter.

Unfortunately, the carbide inverted-cone end mills used for performing the hole-drilling measurements could have a small chamfer at their cutting extremities that generates a small chamfer in the bottom of the hole (**Figure 8**). This small chamfered extremity of the end mill reduces wear and facilitates chip ejection during drilling.

This chamfer influences the strain signals and consequently the calculation of residual stresses. The effect of the hole bottom chamfer has a higher impact on the first depth increments where the chamfer of the end mill generates a hole with a smaller diameter than the nominal diameter. Furthermore, in the case of non-uniform stress distribution, the geometric variation in the hole shape in the first depth increments determines errors not only in the first calculation depths but also in successive calculation depths.

In order to reduce the effect of the hole-bottom chamfer, it is advisable to use a type of cutter with the smallest chamfer available or use the high-speed orbital drilling technique. The method is based on the orbital movement of the end mill as it advances. While producing the same diameter as a center-drilled hole, this technique employs an end mill with a smaller diameter and consequently creates a smaller bottom chamfer.

If the above is not possible, it is necessary to correct the errors generated by the presence of the chamfer.

A first solution for this correction was proposed by Scafidi et al. [17] carrying out an analysis based on the Boundary Element Method. By introducing the gage circle diameter, the drilled hole diameter and the bottom-hole fillet radius, the authors developed a method based on the correction of acquired strains. Subsequently,

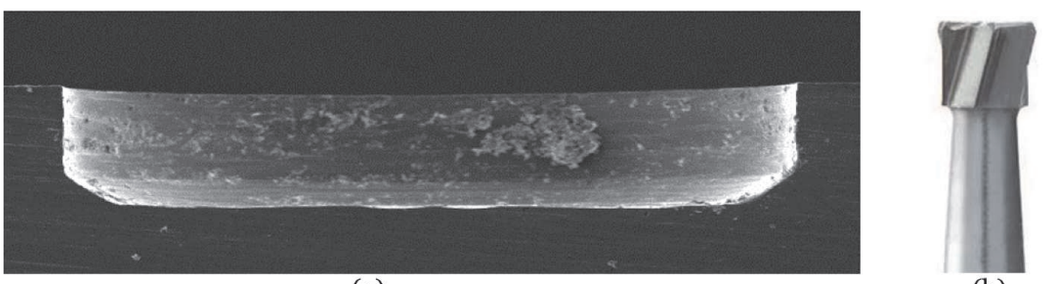

Figure 8.
(a) Section of a drilled hole with a hole-bottom chamfer, (b) Typical carbide inverted-cone end mill used for the hole drilling method.

Blödorn et al. [19] recalculated the ASTM E837 coefficient for blind uniform stress using an FEM model with a hole bottom chamfer.

More recently, the generalized integral method based on the influence functions [8, 9] has been enriched with a new database of displacements, which considers the chamfer as a new geometrical parameter of the finite element model.

For a certain value of the ratio between the height of the hole chamfer and the radius of the drilled hole, this methodology allows the correction of calculated stress for blind holes and non-uniform stress distributions.

Figure 9 shows the finite element model in which the hole bottom chamfer was simulated to evaluate its influence.

The presence of the hole-bottom chamfer influences the calculation of the stresses.

Figure 10 gives an example of the influence of a hole bottom chamfer on the reconstruction of a pure shear stress distribution. In the first part of the depth of the analysis, it is clearly seen that the chamfer determines an under-estimation of the actual stress, especially in the first depth increments. On the contrary, in the second part of the depth of the analysis, the results show an over-estimation of the calculated stresses.

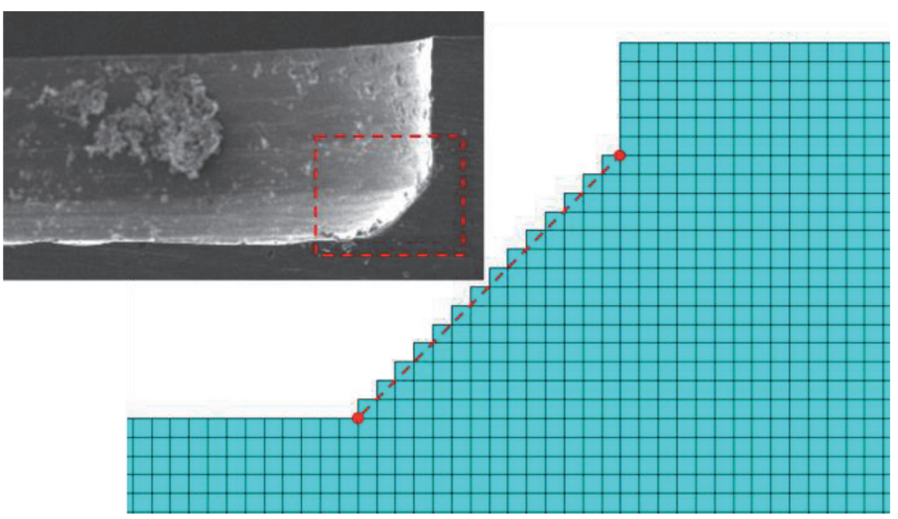

Figure 9.
Finite Element Model used for the evaluation of the calibration coefficients considering the presence of the hole-bottom chamfer.

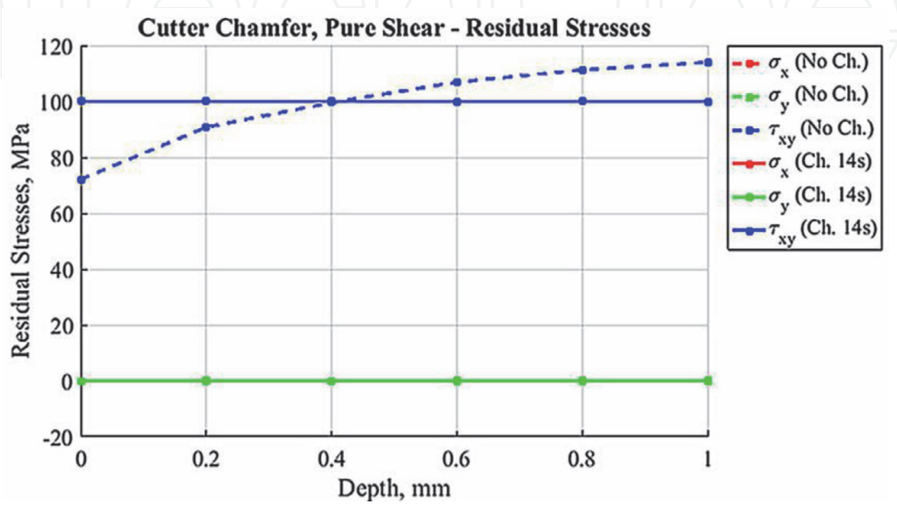

Figure 10.
Residual stresses in the case of pure shear stress, with (dashed line) and without (solid line) the hole-bottom chamfer.

9. Local plasticity limitation: description and possible correction

The ASTM E837 standard reports that satisfactory results can be achieved when measured residual stresses do not exceed about 80% of the yield stress in the case of "thick" workpieces and 50% in the case of "thin" workpieces.

The need for these stress limits is explained by the stress concentration generated by the drilled hole. When a hole is drilled on a loaded workpiece, it generates a stress concentration in the area around the hole. The magnitude of the stress concentration depends on several parameters including the diameter of the drilled hole, the load orientation and the distance of the strain gage grids from the hole. If the stress level is high, localized plastic deformation occurs around the hole, which generates larger overall surface strains (**Figure 11**).

The hole-drilling method requires that the strain gage grids be placed really close to the hole. For this reason, if local plasticity occurs, it may be that the strain measured by the gage is the arithmetical sum of the linear elastic strains and the plastic strains.

In any case, "thick" workpieces are less sensitive to the plasticity effect. This is due to the presence of material in the lower part of the blind hole determining a local reinforcement and reducing the stress concentration factor [3]. This explains the higher measurement limit in the case of a blind hole (80% of σ_Y) compared to the case of a through hole (50% of σ_Y).

Few research studies have been published on this topic to provide possible corrections for this error.

The work of Beghini et al. [20] provides a numerical procedure for correcting the effect of local plasticity in the case of a blind hole for uniform stress calculation. To carry out the stress correction, it is necessary that both the yield stress and the stress–strain curve in the plastic region are defined.

The equivalent stress, corrected to take into account the presence of plasticity σ_{eq}, is evaluated considering the elastic equivalent stress $\sigma_{eq,i}$, the yield stress σ_Y of the material under testing and the plasticity factor f defined as following:

$$f = \frac{\sigma_{eq} - \sigma_{eq,i}}{\sigma_Y - \sigma_{eq,i}} \tag{8}$$

The correction algorithm obviously considers the geometry of the strain gage rosette and therefore the authors provide the calculation coefficients for several strain gage rosettes available on the market.

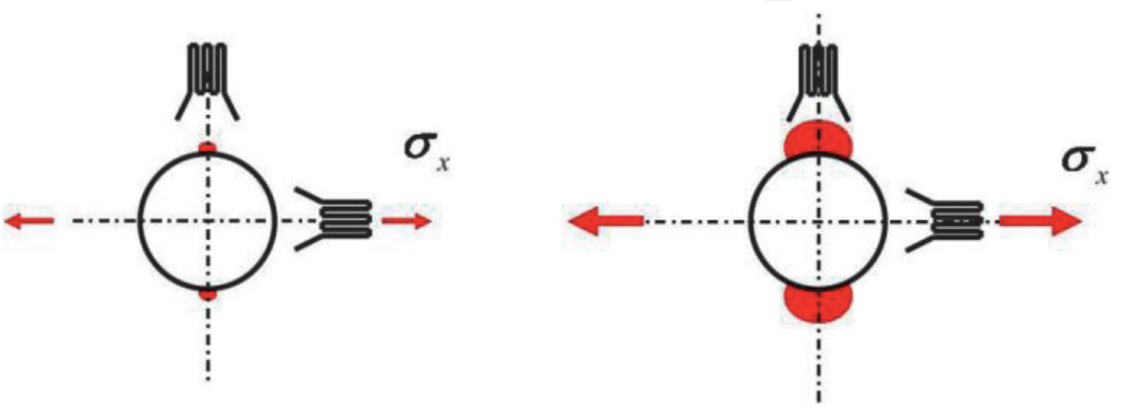

Figure 11.
Local plasticity areas with low applied loads (left side) or high loads (right side).

The previous parameters and FE results are used for the evaluation of the elastically evaluated plasticity factor f_{el}, which is expressed through bivariate polynomials, as a function of the parameters W and μ

$$f_{el} = f + Wf^{\mu} \tag{9}$$

Nobre et al. [21] provide a similar approach for the estimation of the plasticity factor f. The material characteristics are taken into account by measuring the variation of Vickers hardness, which estimates the material strain hardening due to the increase of plastic deformation.

Plasticity generates a non-linearity on strain measurements.

Beghini et al. [22] propose a special 4-grid strain gage rosette for the correction of the plasticity effect, which is available on the market (HBM). The correction is valid for the standard 3-grid rosettes only if the perpendicular grids are oriented in the directions of the principal strains.

10. Evaluation of uncertainty

The evaluation of uncertainties associated with measurement of residual stresses by the hole-drilling method is a topic that has been little investigated. The evaluation, mainly in the case of non-uniform stress fields, involves a large number of parameters from different sources, including the properties of the materials under testing, the strain readings and the hole execution methods.

Standard ASTM E837-13a [1] contains only some basic information about precision and bias associated with the hole-drilling measurement method, mainly in the case of uniform stress calculation. In fact, the standard states that the bias associated with a residual stress measurement by the hole-drilling method is less than ±10% when dealing with uniform residual stresses. Based on the results of round-robin test programs, the precision (random error) is such as to give a standard deviation of ±14 MPa for AISI 1018 carbon steels and a standard deviation of ±12 MPa for type AISI 304 stainless steels. The standard also reports that the uncertainties in the case of non-uniform stress measurements are expected to be much larger than for uniform stress measurements.

One of the first papers on the subject of evaluation of uncertainty was published by Oettel [25] (UNCERT Code of Practice 15). The work proposes an approach for the evaluation of hole-drilling uncertainty in the case of uniform stress fields and takes into account typical errors in the determination of material properties, errors in the measurement of acquired strains, the hole diameter and the influence of calculation coefficients. The code of practice can be applied only to uniform residual stress calculation equations based on ASTM E837-95 and cannot be used with the current version of the ASTM standard [1].

Scafidi et al. [26] further developed this methodology by applying it to the recent version of the average uniform stress calculation and considering additional parameters, such as the step-by-step drilling depth.

Regarding evaluation of uncertainty in the case of non-uniform stresses, the first approach was provided by Schajer et al. [24] based on the Integral method. They consider a number of input estimates including the properties of materials (i.e. Young's modulus), strain readings, hole diameter and hole depths. The uncertainty components have statistical normal distributions with zero mean and are independent of each other and each one is linearly combined.

The uncertainties of the measured strains are considered as an input, but fixed for each step.

More recently a new approach was proposed by Peral et al. [27], based on a Monte Carlo analysis of the influence of the main parameters affecting the measurements. The methodology takes into account a higher number of parameters compared to the approach proposed by Schajer. In particular, the uncertainty components due to Poisson's ratio and identification of the zero-depth are also considered. The authors demonstrated that their method is comparable with the approach of Schajer et al. [24], showing generally more conservative results although in good agreement.

SINT Technology recently developed another approach to evaluation of uncertainty, based on the GUM methodology [23], and it is implemented in the calculation software EVAL 7.

Before calculation of uncertainties, all possible systematic errors are corrected, in particular those determined by eccentricity (Section 6), intermediate thickness (Section 7), hole bottom chamfer (Section 8) or local plasticity in the case of uniform stress calculation (Section 9).

The uncertainties determined by the following input parameters are considered: Young's modulus, Poisson's ratio, hole diameter, accuracy of the strain measurement system, zero depth offset error, depth of drilling increments.

This approach can be applied to all available calculation methods including the ASTM standard: clearly, the generalized integral method approach (Section 4) is preferable as it allows several systematic errors to be corrected (Sections 6–8).

The functional relationship f that connects the output estimate to the inputs and the measurements can be written, for each calculation step j, as:

$$\sigma_{MIN,MAX}, \beta = f\left(\mathrm{E}, \nu, \mathrm{D}_0, \varepsilon_{1,\mathrm{j}}, \varepsilon_{2,\mathrm{j}}, \varepsilon_{3,\mathrm{j}}, \mathrm{z_j}, \mathrm{z}_0\right) \tag{10}$$

where E is the Young's modulus of the material; ν the Poisson's ratio; D_0 the diameter of the drilled hole; $\varepsilon_{1,\mathrm{j}}, \varepsilon_{2,\mathrm{j}}, \varepsilon_{3,\mathrm{j}}$ the Readings of the strain gage grids for the step j; $\mathrm{z_j}$ the depth advance for the step j and z_0 the depth error during the zero-depth determination.

The reading of the strain gage grids, for each calculation step j and for each channel y, is derived from the following parameters:

$$\varepsilon_{1,\mathrm{j}}, \varepsilon_{2,\mathrm{j}}, \varepsilon_{3,\mathrm{j}} = f(\mathrm{K_x}, (\Delta V/V)_{j,x} \tag{11}$$

where $\mathrm{K_x}$ is the Gage Factors of the strain gage for each grid x; $(\Delta V/V)_{j,x}$ is the electrical signal output for each channel x and for each step j.

The uncertainty on the electrical output $(\Delta V/V)_{j,x}$ depends on the strain gage amplifier technical specifications, such as class of accuracy or resolution, linearity and noise to signal ratio. This information can be obtained from the technical datasheet of the strain gage amplifier.

Also the uncertainty on the measurement of the drilled hole D_0 and the depth increments $\mathrm{z_j}$, for each j step, are evaluated starting from the technical specification respectively of the dial gages used for the hole measurements and the mechanical drilling unit that makes the hole.

The uncertainty component due to the temperature variation during testing is considered negligible as the strain gages are self-compensated and a three-wire half-bridge connection is adopted to minimize the effect of temperature on the cables. Also the uncertainties due to the Influence Functions are considered negligible. **Table 3** shows the typical input parameters taken into account for the evaluation of the uncertainty, along with the type of statistical distribution.

Assuming that all the input quantities are independent, the combined standard uncertainty, for each calculation step j, is given by:

Input estimates x_i	Description	Sub-input estimates	Distribution	Origin
E	Young's Modulus of the materials under testing	/	Rectangular	Material datasheet
ν	Poisson's ratio of the materials under testing	/	Rectangular	Material datasheet
D_0	Diameter of the drilled hole	/	Normal	Resolution of the dial gages
				Max. error of the dial gages
				Repeatability of the dial gages
$\varepsilon_{1,j}, \varepsilon_{2,j}, \varepsilon_{3,j}$	Gage factor of the strain gage grids	K_x for each channel x	Normal	Uncertainty declared on the strain gage datasheet
	Electrical output of each strain gage grid	$(\Delta V/V)_{j,x}$ for each channel x for each step j	Normal	Class of accuracy of the strain gage amplifier
				Linearity of the strain gage amplifier
				Resolution of the strain gage amplifier
				Noise of the strain gage amplifier
z_j	Depth increment	/	Normal	Resolution of the hole-drilling mechanical device
				Max. error between two consecutive steps of the hole-drilling mechanical device
z_0	Zero-depth error	/	Rectangular	Datasheet of the hole-drilling mechanical device

Table 3.
Parameters used for the uncertainty evaluation and distribution of probability.

$$u_c(y) = \sqrt{\sum_{I=1}^{N} \left(\frac{\partial f}{\partial x_I}\right)^2 u^2(x_I)} \tag{12}$$

where y is the measurement result (output estimate); $u_C(y)$ is the combined standard uncertainty for measurement result; x_I the input quantity measurement (input estimate); $u(x_I)$ is the standard uncertainty for each input quantity; $I = 1, \ldots, N$ is the number of input quantities.

Finally, the expanded uncertainty U is obtained by multiplying the combined standard uncertainty $u_C(y)$ by a coverage factor k:

$$U = ku_C(y) \tag{13}$$

The result of a measurement is then conveniently expressed as:

$$Y = y \pm ku_C(y) \tag{14}$$

The advantage of this method is the capability to numerically evaluate, for each parameter and for each calculation depth, the first derivatives of the functional

relation f (sensitivity coefficients) which, in the formula (12), multiply the standard uncertainty square $u(x_i)$ of each input estimate x_i.

This calculation procedure, which is implemented in the EVAL 7 software, requires the execution of a high number of stress calculations for the uncertainty evaluation related to hole drilling measurements.

In particular, considering a measurement carried out according to the ASTM standard using 20 calculation depths, the uncertainty evaluation requires the repetition and therefore the combination of the results obtained with 206 different stress calculations.

11. Experimental validation of the method on a four-point bending rig

The entire measurement chain and the testing parameters (rotational speed, type of end mill, feed rate and delay time) were verified using a special apparatus, developed by SINT Technology, which applies a known bending stress on a specially designed specimen.

The specimen is a flat rectangular cross section cantilever beam, fixed at one end, and loaded at the other end by means of a pneumatic actuator (**Figure 12**).

The material used for the specimen is aluminum alloy AW7075 T651. The maximum applied bending stress was approximately 25 MPa.

An approximately 1.90 mm hole diameter was drilled with 130 incremental drilling depths of 10 μm up to a 1.30 mm total depth. The rotational speed was approx. 400,000 rpm and the feed rate 0.2 mm/min. To prevent any interaction between the tip and the specimen, the cutter was fully raised for each drilling step. The diameter was accurately measured after drilling, for each test, with the microscope installed on the system and two dial gages, also to determine the residual eccentricity.

The (uniaxial) stress due to bending was easily obtained from the beam theory, **Figure 12b**, Eq. 15:

$$\sigma_{Be} = 6\,\frac{Fb}{wh^2} \tag{15}$$

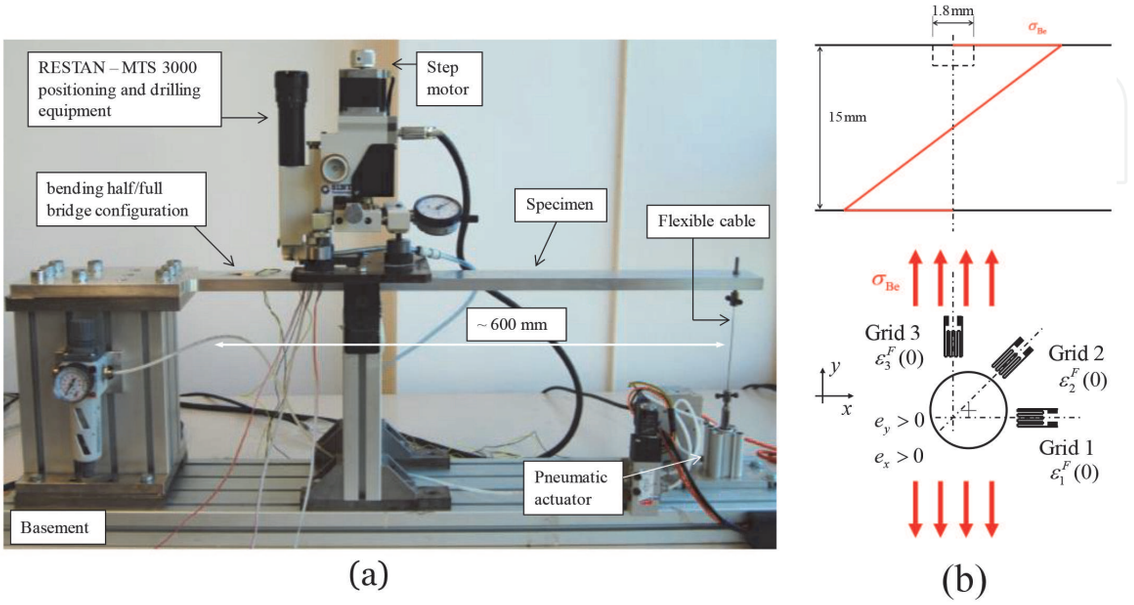

Figure 12.
(a) Bending test bench to simulate a known reference residual stress and (b) shows the linear distribution of the bending stress and orientation of the strain gage rosette grids and hole eccentricity definition.

where b is the distance between the load axis and the rosette strain gage center, wh^2 is the width and height of the beam cross section, and F is the load imposed by the pneumatic actuator.

A known load was used for determining the properties of the material. In fact, the elasticity parameters (Young's modulus E and Poisson's ratio ν) of the material were measured before drilling by applying a preliminary bending load before drilling.

Grid 1 of each strain gage should be aligned with the beam axis. The manual strain gage installation unavoidably introduces a misalignment. However, the angle between grid 1 and the beam axis can be found from Eq. 16 (accurate approximation for small values of γ):

$$\gamma = \frac{1}{2} \cdot \frac{\varepsilon_1^F(0) - 2\varepsilon_2^F(0) + \varepsilon_3^F(0)}{\varepsilon_1^F(0) - \varepsilon_3^F(0)} \tag{16}$$

The measured strains need to be decoupled in order to deduce the relaxed strain due to the bending stress. The relaxed strains due to the residual stresses and the relaxed strains due to the bending stresses are obtained as:

$$\begin{aligned} \varepsilon_i^{RS}(z_j) &= \varepsilon_i(z_j) \\ \varepsilon_i^{Be}(z_j) &= \varepsilon_i^F(z_j) - \varepsilon_i(z_j) - \varepsilon_1^F(0) \end{aligned} \tag{17}$$

Strain $\varepsilon_i^F(0)$ needs to be subtracted in the second member of Eq. 17 since the relaxed strains are defined as the effect of introduction of the drilled hole, therefore they need to be zero at zero depth. Finally, the experimental data are the bending relaxed strains as a function of hole depth increments $\varepsilon_i^{Be}(z_j)$.

12. Test results and analysis

The following testing conditions were adopted during the measurements.

- Surface bending stress (σ_{Be}): 24.8 MPa
- Strain gage rosette: CEA-062UM-120
- Measured eccentricity radius: 0.02 mm
- Measured eccentricity angle: 135°

The following parameters were then used for the stress calculation and for the uncertainty evaluation:

- Young's modulus (E): 71000 ± 3550 MPa
- Poisson's ratio (ν): 0.33 ± 0.01
- Hole diameter (D_0): 1.88 ± 0.01 mm
- Gage factor uncertainty (K): 1%
- Uncertainty on the maximum electrical output ($\Delta V/V$): ±0.50 μm/m

- Zero-depth uncertainty (z_0): ±0.005 mm
- Depth measurement uncertainty (z): ±0.01 mm

After performing the drilling tests, the relaxed strains were imported into the EVAL 7 calculation software developed by SINT Technology. The calculation of non-uniform stresses was carried out according to the following two methods: the original ASTM 837-13a standard and the generalized integral method, based on the Influence Functions, by applying the algorithms described in the previous sections and correcting some systematic errors.

The extended features are shown in **Table 4**.

The stresses were calculated considering a distribution of 20 constant steps within 1 mm of depth.

Next, the bending stress distribution was calculated by the generalized integral method and then compared with the expected bending stress distribution.

Finally, based on the calculated stress curves, the uncertainty of measurement was evaluated considering the input quantities reported above (Section 12). The measurement uncertainties are expressed as standard uncertainties multiplied by a coverage factor equal to 2 (which in the case of normal distribution corresponds to a confidence level of about 95%).

Figure 13 compares the expected bending stresses with the stress components σ_x, σ_y and τ_{xy}, calculated from the interpolated relaxed strains with their associated uncertainty.

The purpose of the authors is to highlight the importance of the correction of each source of error, which is not contemplated in the ASTM E837 calculation. This has been achieved by showing the effects on the calculated stresses in the event that those corrections are not considered. For this reason, one by one, all the corrections have been deselected from the generalized integral method with all the active corrections.

Figure 14 shows the percentage error on σ_{Be} when the generalized integral method is not applied, due to the hole eccentricity, the combination of Poisson's ratio and the hole diameter, and the geometry of the strain gage rosette.

Regarding eccentricity, a maximum error of approximately 1.5% is committed, in the area closest to the surface. It is necessary to highlight that the eccentricity radius error, that affects this data, is similar to the maximum value tolerated by the ASTM 837-13a standard. In some real cases, due to the inexperience of the operator

Features	**Comparison**	
	ASTM E837-13a	**Generalized integral method, based on the influence functions**
Eccentricity correction	Not available	Available
Applicability to strain gage rosettes	Only to rosettes listed in the standard	To any rosette available in the market
Poisson's ratio correction	Approximate	Complete
Hole diameter correction	Approximate	Complete
Hole-bottom chamfer correction	Not available	Available
Intermediate thickness extension	Not available	Available
Tikhonov regularization	Available	Available

Table 4.
Comparison between the ASTM E837 & generalized integral method, based on the influence functions.

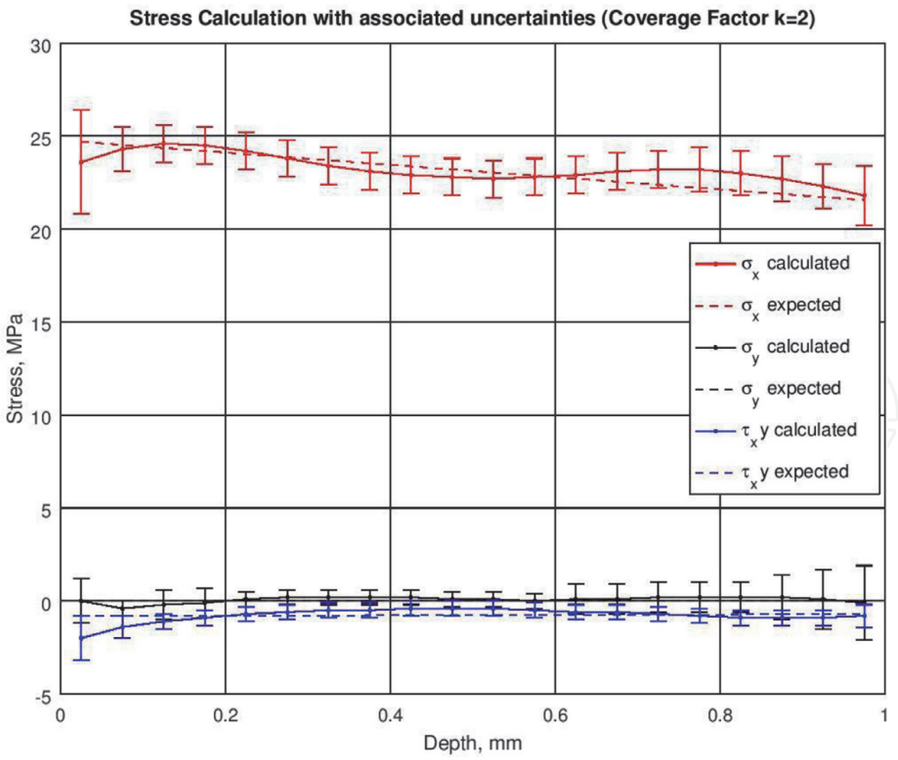

Figure 13.
Comparison between expected bending stresses and the calculated stress components.

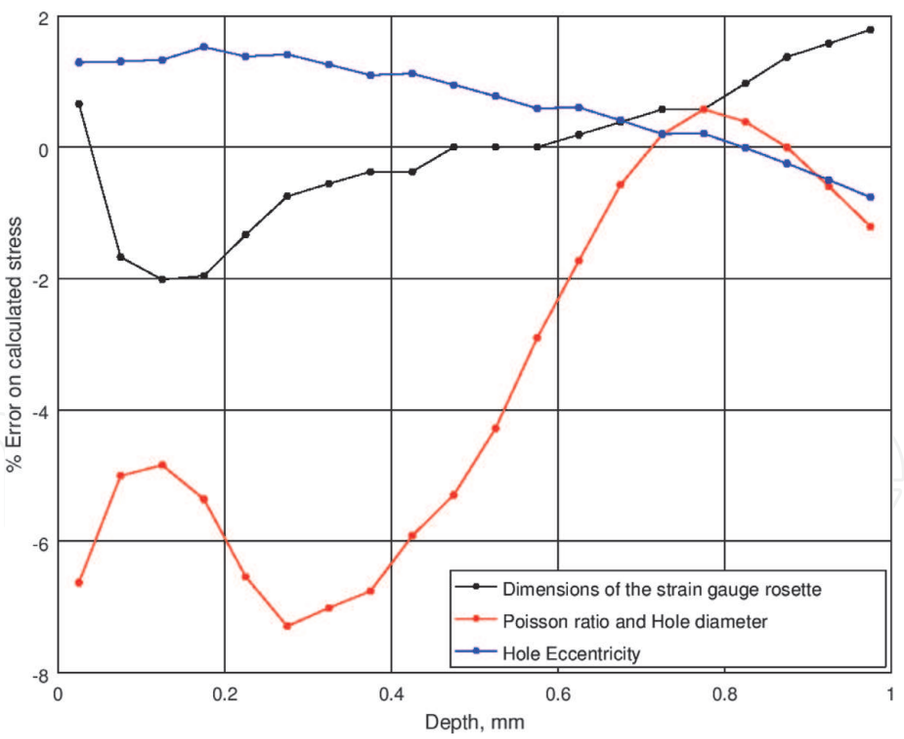

Figure 14.
Percentage error on σ_{Be} when the generalized integral method is not applied.

or to non-standard test conditions, the eccentricity radius can be higher than the limitation reported by the standard and, therefore, correction of eccentricity is essential for an accurate evaluation of residual stresses.

Regarding the influence of Poisson's ratio and the hole diameter, the maximum deviation is around 8%. Indeed, the calibration constants are not

expressed as a function of Poisson's ratio and the diameter of the measured hole: only the approximate correction is provided. In this case, both the measured diameter (D = 1.88 mm) and the Poisson's ratio considered (n = 0.33 mm) are far from those used to generate the calibration matrices reported in the standard.

Finally, regarding the influence of the geometry of the strain gage rosette, the maximum deviation is approximately 2%. It represents the error due to use of a rosette that is different from the geometry envisaged in the standard. In this case, the rosette that was used is very similar to type B of the standard. In other cases, the errors may be higher.

13. Conclusions

The paper describes some improvements in the hole-drilling test method for the analysis of residual stresses, developed to increase accuracy. These improvements have been introduced to overcome some limitations and correct some errors that can derive from the direct application of the ASTM E837-13a standard.

To make calculation of the distribution of non-uniform stresses more accurate, the evaluation of residual stresses was carried out by applying the general method, based on the influence functions, proposed by Beghini et al. [8, 9]. This approach is more extensive with respect to the integral method proposed by Schajer [13, 14] and can include a dependency on a higher number of parameters. This more general approach avoids some errors and removes some limitations in the evaluation of non-uniform residual stresses deriving from the application of the ASTM E837-13a standard, which is based on the Integral method. Ultimately, the Integral method can be considered as a special case of the influence function method in which piecewise constant functions are used as the basis.

With this approach, some limitations of the standard can be overcome and, in particular, applicability of the hole-drilling test method is extended:

- For all strain gage rosettes available on the market, instead of just the A, B and C type rosettes [1],
- When eccentricity of the hole is greater than 0.004 D
- When the thickness s of the workpiece is between $0.2D < s \leq 1.0D$.

Furthermore, with this approach it will be possible to correct errors due to:

- hole eccentricity
- hole bottom chamfer
- approximate correction if the hole diameter and Poisson's ratio differ from the nominal value used for the evaluation of the calibration coefficients in ASTM
- local plasticity, only in the case of blind holes and uniform stress

The paper also describes developments in measurement instrumentation with the use of automatic systems instead of manual systems and a procedure for evaluating measurement uncertainties in the case of non-uniform distribution, based on the GUM method.

All the features reported above have been introduced in dedicated software for the evaluation of residual stresses and related uncertainty. Finally an experimental test, performed on a 4-point bending test rig, is described.

List of symbols

σ_x	residual stress normal component in the x direction [MPa]
σ_y	residual stress normal component in the y direction [MPa]
τ_{xy}	residual stress shear component in the xy plane [MPa]
σ_{MIN}	minimum principal residual stress [MPa]
σ_{MAX}	maximum principal residual stress [MPa]
β	principal angle [rad]
σ_Y	yield stress of the testing material [MPa]
D	diameter of the strain gage circle [mm]
D_0	diameter of the drilled hole [mm]
D_N	ASTM E837 nominal hole diameter [mm]
G_L	grid length [mm]
G_W	grid width [mm]
$\varepsilon_1, \varepsilon_2, \varepsilon_3$	strains acquired from the strain gage rosette [μm/m]
p, q, t	combination strain [μm/m]
P, Q, T	combination stress [MPa]
E	Young's modulus [MPa]
ν	Poisson's ratio
$\bar{a}, \bar{b}$	calibration constants used in the calculation of uniform stress
s	workpiece thickness [mm]
n	number of acquisition steps
j	number of hole depth steps
k	sequence number for hole depth steps
$\bar{\mathbf{a}}, \bar{\mathbf{b}}$	calibration matrix constants used in the calculation of non-uniform stress
c	Tikhonov regularization matrix
$\boldsymbol{\alpha_P}, \boldsymbol{\alpha_Q}, \boldsymbol{\alpha_T}$	Tikhonov regularization factors
$\bar{a}_{j,k}, \bar{b}_{j,k}$	calibration matrix for isotropic and shear stresses
S	vector of the stress components
e	vector of the strain components
$\bar{\boldsymbol{A}}$	generalized matrix of calibration coefficients
C	generalized Tikhonov regularization matrix
e_x, e_y	eccentricity component of the x and y directions
$\sigma_{eq,el}$	equivalent stress [MPa] corrected for plasticity effect
$\sigma_{eq,i}$	equivalent residual stress producing the onset of plasticity in the 2D case
f, f_{el}	plasticity factor calculated in plastic and elastic field
W, μ	coefficients for the plasticity correction
z_j	depth increment j
z_0	depth error during the zero-depth determination
K_x	gage factors of the strain gage for each grid x (x = 1,2,3)
$(\Delta V/V)_{j,x}$	electrical output reading for each grid x (x = 1,2,3) and for each depth increment j
y	measurement result (output estimate)
$u_C(y)$	combined standard uncertainty for measurement result

x_I	input quantity measurement (input estimate)
$u(x_I)$	standard uncertainty for each input quantity
I	number of input quantities

Author details

Emilio Valentini*, Lorenzo Bertelli, Alessio Benincasa and Simone Gulisano
SINT Technology S.r.l., Florence, Italy

*Address all correspondence to: emilio.valentini@sintechnology.com

References

[1] ASTM E837-13a. Standard Test Method for Determining Residual Stresses by the Hole-Drilling Strain-Gage Method. West Conshohocken, PA: ASTM International, West Conshohocken; 2013. Available from: www.astm.org

[2] Valentini E, Bertelli L, Benincasa A. Improvements in the hole-drilling test method for determining residual stresses in polymeric materials. Materials Performance and Characterization. 2018;7(4):446-464. DOI: 10.1520/MPC20170123 ISSN 2379-1365

[3] Schajer GS, Whitehead PS. Hole-Drilling Method for Measuring Residual Stress. Vermont, USA: Morgan & Claypool; 2018. 186 pp

[4] Schajer GS, Whitehead PS. Hole-drilling and ring coring. In: Schajer GS, editor. Chapter 2 in Practical Residual Stress Measurement Methods. Chichester, UK: Wiley; 2013. pp. 29-64

[5] Schajer GS. Measurement of non-uniform residual stresses using the hole-drilling method. Part I—Stress calculation procedures. Journal of Engineering Materials and Technology. 1988;**110**:338-343

[6] Schajer GS. Measurement of non-uniform residual stresses using the hole-drilling method. Part II—Practical application of the integral method. Journal of Engineering Materials and Technology. 1988;**110**:344-349

[7] Alegre JM, Díaz A, Cuesta II, Manso JM. Analysis of the influence of the thickness and the hole radius on the calibration coefficients in the hole-drilling method for the determination of non-uniform residual stresses. Experimental Mechanics. 2019;**59**:79. DOI: 10.1007/s11340-018-0433-0

[8] Beghini M, Bertini L, Mori LF. Evaluating non-uniform residual stress by the hole-drilling method with concentric and eccentric holes. Part I. Definition and validation of the influence functions. Strain. 2010;**46**: 324-336. DOI: 10.1111/j.1475-1305.2009.00683.x

[9] Beghini M, Bertini L, Mori LF. Evaluating non-uniform residual stress by the hole-drilling method with concentric and eccentric holes. Part II: Application of the influence functions to the inverse problem. Strain. 2010;**46**: 337-346. DOI: 10.1111/j.1475-1305.2009.00684.x

[10] Beghini M, Bertini L, Santus C, Benincasa A, Bertelli L, Valentini E. Validazione sperimentale di una rosetta a 6 griglie per ridurre l'errore di eccentricità nella misura delle tensioni residue. In: Congresso AIAS XXXIX; Maratea (PZ). 2010. ISBN: 8860930749

[11] Nau A, Scholtes B. Experimental and numerical strategies to consider hole eccentricity for residual stress measurement with the hole drilling method. Materials Testing. 2012;**54**(5): 296-303. DOI: 10.3139/120.110330

[12] Ajovalasit A. Measurement of residual stresses by the hole-drilling method: influence of hole eccentricity. Journal of Strain Analysis for Engineering Design. 1979;**14**:171-178

[13] Barsanti M, Beghini M, Bertini L, Monelli BD, Santus C. First-order correction to counter the effect of eccentricity on the hole-drilling integral method with strain-gage rosettes. The Journal of Strain Analysis for Engineering Design. 2016;**51**(6):431-443. DOI: 10.1177/0309324716649529

[14] Peral D, Correa C, Diaz M, et al. Measured strains correction for

eccentric holes in the determination of non-uniform residual stresses by the hole drilling strain gage method. Materials & Design. 2017;**132**:302-313. DOI: 10.1016/j.matdes.2017.06.051

[15] Abraham C, Schajer GS. Hole-drilling residual stress measurement in an intermediate thickness specimen. In: Experimental and Applied Mechanics. Vol. 4. Conference Proceedings of the Society for Experimental Mechanics Series. New York, NY: Springer; 2013. Available from: https://doi.org/10.1007/978-1-4614-4226-4_46

[16] Beghini M, Bertini L, Giri A, Santus C, Valentini E. Measuring residual stress in finite thickness plates using the hole-drilling method. The Journal of Strain Analysis for Engineering Design. 2019;**54**(1):65-75. DOI: 10.1177/0309324718821832

[17] Scafidi M, Valentini E, Zuccarello B. Effect of the hole-bottom fillet radius on the residual stress analysis by the hole drilling method. In: ICRS-8 The 8th International Conference on Residual Stress; Denver. 2008. pp. 263-270

[18] Simon N, Gibmeier J. Consideration of tool chamfer for realistic application of the incremental hole-drilling method. Materials Research Proceedings. 2017;**2**: 473-478. DOI: 10.21741/9781945291173-80

[19] Blödorn R, Bonomo L, Viotti M, Schroeter R, Albertazzi A Jr. Calibration coefficients determination through FEM simulations for the hole-drilling method considering the real hole geometry. Experimental Techniques. 2017;**41**:37. DOI: 10.1007/s40799-016-0152-3

[20] Beghini M, Bertini L, Santus C. A procedure for evaluating high residual stresses using the blind hole drilling method, including the effect of plasticity. The Journal of Strain Analysis for Engineering Design. 2010;**45**(4): 301-318. DOI: 10.1243/03093247JSA579

[21] Nobre JP, Kornmeier M, Scholtes B. Plasticity effects in the hole-drilling residual stress measurement in peened surfaces. Experimental Mechanics. 2018;**58**:369. DOI: 10.1007/s11340-017-0352-5

[22] Beghini M, Santus C, Valentini E, Benincasa A. Experimental verification of the hole drilling plasticity effect correction. Materials Science Forum. 2011;**681**:151-158. DOI: 10.4028/www.scientific.net/MSF.681.151

[23] JCGM 100. Evaluation of measurement data—Guide to the expression of uncertainty in measurement. ISO/IEC Guide 98-3. 2008

[24] Schajer GS, Altus EE. Stress calculation error analysis for incremental hole-drilling residual stress measurements. ASME Journal of Engineering Materials and Technology. 1996;**118**(1):120-126. DOI: 10.1115/1.2805924

[25] Oettel R. The determination of uncertainties in residual stress measurement (using the hole drilling technique). Code of Practice. EU Project No. SMT4-CT97-2165. Sept. 2000;**15**(1)

[26] Scafidi M, Valentini E, Zuccarello B. Error and uncertainty analysis of the residual stresses computed by using the hole drilling method. Strain. 2011;**47**: 301-312. DOI: 10.1111/j.1475-1305.2009.00688.x

[27] Peral D, de Vicente J, Porro JA, Ocaña JL. Uncertainty analysis for non-uniform residual stresses determined by the hole drilling strain gage method. Measurement. 2017;**97**:51-63. ISSN: 0263-2241. DOI: 10.1016/j.measurement.2016.11.010